Solvent Polarity and Dopant Effect on the Electronic Structure of the Emeraldine Salt

ARTICLE *in* INTERNATIONAL JOURNAL OF QUANTUM CHEMISTRY · FEBRUARY 2011

Impact Factor: 1.43 · DOI: 10.1002/qua.22703

4 AUTHORS, INCLUDING:

J. Romanova
University of Surrey
18 PUBLICATIONS **106** CITATIONS
SEE PROFILE

Galia Madjarova
Sofia University "St. Kliment Ohridski"
24 PUBLICATIONS **253** CITATIONS
SEE PROFILE

A. Tadjer
Sofia University "St. Kliment Ohridski"
65 PUBLICATIONS **425** CITATIONS
SEE PROFILE

Solvent Polarity and Dopant Effect on the Electronic Structure of the Emeraldine Salt

JULIA ROMANOVA,[1,2] GALIA MADJAROVA,[1] ALIA TADJER,[1] NATALIA GOSPODINOVA[2,3,4]

[1]*Laboratory of Quantum and Computational Chemistry, Faculty of Chemistry, University of Sofia, 1 James Bourchier Ave., 1164 Sofia, Bulgaria*

[2]*Université de Haute Alsace, Faculté des Sciences et Techniques, 2 rue des Frères Lumière, 68093, Mulhouse Cedex, France*

[3]*Institut de Science des Matériaux de Mulhouse (LRC 7228), Carbones et Matériaux Hybrides, 15 rue Jean Starcky, BP 2488, 68057, Mulhouse Cedex, France*

[4]*Ecole Nationale Superieure de Chimie de Mulhouse, Matériaux et Polymères, 3 rue Alfred Werner, 68093, Mulhouse Cedex, France*

Received 15 January 2010; accepted 25 February 2010
Published online 29 June 2010 in Wiley Online Library (wileyonlinelibrary.com).
DOI 10.1002/qua.22703

ABSTRACT: Quantum mechanical simulations of a variety of inorganic and organic emeraldine salts (doping agents HCl, HBr, H_2SO_4, MSA, BSA, and CSA) in bipolaron and polaron form with account of solvents of different polarity (chloroform, *m*-cresol, and water) are reported for the first time. The models are based on tetramers, and the calculations are performed with the DFT method. The polarizable continuum model is used for the treatment of solute–solvent interaction. The effect of the different dopants and polarity of the solvents on the electronic structure and properties of the salts is evaluated and interpreted from the standpoint of the available experimental data. Int J Quantum Chem 111: 435–443, 2011

Key words: DFT; PCM; polyaniline; inorganic/organic dopants; solvent effect

Correspondence to: A. Tadjer; e-mail: tadjer@chem.uni-sofia.bg

Contract grant sponsor: Bulgarian National Science Fund.
Contract grant numbers: BYX-202/06, DO-02-136/08, DO-02-82/08.
Contract grant sponsor: Science Fund of the University of Sofia.
Contract grant number: SU-185/2009.
Contract grant sponsor: French Government (PhD "Cotutelle" Fellowship).

Additional Supporting Information may be found in the online version of this article.

Introduction

Polyaniline (PANI) features an unusual combination of conducting [1], optical [2], and mechanical [3] properties and is one of the most intensely investigated polymers [4]. PANI exists in three basic oxidation states: leukoemeraldine, emeraldine, and pernigraniline. Prime interest attracts the emeraldine base (Fig. 1,A), as the conducting form of the polymer is obtained from its solutions at low pH in the presence of acids (protonating agents) [5]. The process, known as proton acid doping, is specific for PANI and is essentially a reversible insulator–metal transition [1(a)]. In agreement with the experimentally observed changes and the quantum chemistry modeling, a mechanism of the emeraldine salt formation in aqueous solution has been suggested [6].

The imine nitrogen atoms in the repeating unit (RU) of the polyemeraldine base are deemed to be the protonation targets in the first stage (Fig. 1: A → B) of the process. The protonated sites are electrostatically neutralized by the acid counterions. At this stage, the emeraldine salt is in its bipolaron form (Fig. 1,B). The latter is characterized by a singlet tetramer RU, bearing two positive charges on the organic skeleton, with most prominent electron deficiency at the quinoid ring. In the next stage (Fig. 1: B → C), however, the bipolaron form may undergo a transformation (internal redox reaction) resulting in polarons formation (Fig. 1,C). Upon separation of the polarons, a polaron lattice is formed, that is, the stable polaron form of the emeraldine salt (Fig. 1,D). The RU of the polaron lattice is a dimer, accommodating one unpaired spin and carrying one positive charge on the organic moiety. The molecular-level studies of the polaron form render explanation of some intrinsic properties of the conducting PANI: the presence of EPR signal and relatively small energy gap. The obtaining of polaron or bipolaron form depends on a number of factors, such as the polymer molecular weight and supramolecular organization. For instance, it has been demonstrated experimentally that short oligomers (e.g., phenyl-capped tetramers) of the emeraldine salt exist in the bipolaron form [7]. On the other hand, as mentioned above, studies of magnetic susceptibility and optical measurement on the polyemeraldine salt suggest a polaron lattice [1, 6].

It has been shown experimentally that conducting emeraldine salt can be prepared by doping of

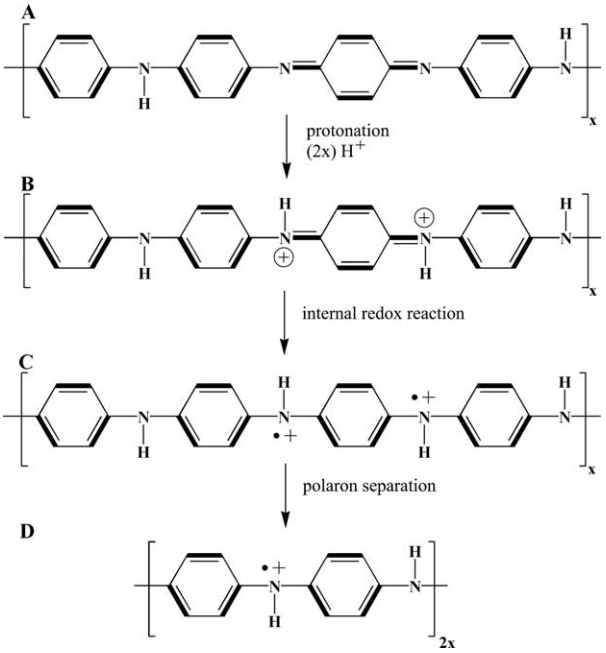

FIGURE 1. Transformations of polyemeraldine after 50% protonation. (A) Emeraldine base; (B) bipolarons and (C) polarons formation in emeraldine salt; and (D) polarons separation, which results in polaron lattice formation (the idea borrowed from Ref. [6]).

the base with various mineral acids: HCl, HBr, HNO_3, and H_2SO_4 [8], and organic acids: methylsulfonic acid (MSA), benzenesulfonic acid (BSA), dodecylbenzenesulfonic acid (DBSA), *p*-toluenesulfonic acid (TSA), and camphorsulfonic acid (CSA) [9]. The interaction emeraldine base/dopant is phenomenologically the *primary doping*. MacDiarmid and Epstein introduced the term primary dopant defining it as: "a substance, a relatively small quantity of which drastically changes the electronic, optical, magnetic, and/or structural properties of the polymer … accompanied by a large increase in conductivity" [10]. Depending on the dopant type, the preparation of emeraldine salt in solution is carried out in solvents of different nature and polarity, for example, water, chloroform, and *m*-cresol. It has been established that the nature of the solvent (or mixture of solvents) is crucial for the conducting and optical characteristics of the emeraldine salt [7]. The conductivity may vary in a broad range of values even when the same primary dopant is applied; for instance, emeraldine-CSA salt in chloroform may feature conductivity of 10^{-1} S/cm, whereas in *m*-cresol it is in the interval 100–400 S/cm. To explain the

observed phenomenon, the notion of *secondary doping* has been introduced. The secondary dopant is defined as "an apparently 'inert' substance that, when applied to a primary-doped polymer, induces still further changes in the above properties including a further increase in conductivity. It differs from a primary dopant, in that the newly enhanced properties may persist even upon complete removal of the secondary dopant" [10]. Among the aforementioned solvents, *m*-cresol plays the role of an efficient secondary dopant. The authors interpret its effect promoting the idea that the chemical nature of the solvent makes it a "good solvent" for the PANI salt as it solvates better the polymer chain and/or the counterions, has relatively high polarity, and participates in π-stacking with the chain and H-bonding. This complex assortment of properties is atypical for water or chloroform. The secondary dopant changes the polymer conformation to a more stretched one, decreases the number of imperfections along the π-conjugated chain, and improves the bulk (predominantly the intramolecular) conductivity.

The above clearly indicates that the dopant–PANI–solvent interaction has a fairly complex nature and is of particular importance for the properties of conducting polymers. Therefore, quantum chemistry assessment of the system would allow detailed clarification of the relationships therein and more specifically would aid the search of new appropriate conductivity-boosting dopant–solvent pairs. Because of the large size of the system, modeling of explicit interactions primary dopant/PANI with implicit treatment (polarizable continuum) of the secondary dopant is the most feasible initial step of a study at the *ab initio* level. To this end, calculations of tetramer emeraldine salts obtained with an ample set of inorganic and organic primary dopants in implicit medium of three different solvents are performed in this study. The simulations are carried out with the BLYP/6-31G*/polarizable continuum model (PCM) method. Both the bipolaron (singlet) and the polaron (triplet) forms of each salt are considered. The doping effect on the emeraldine base and the influence of the primary dopant and environment polarity are quantified. To our knowledge, such a wide-spectrum theoretical investigation of the PANI–dopants interaction has not been reported, and we believe that this communication will add a new perspective to the understanding of this complex system.

Model and Computational Protocol

Over the years, PANI has been treated with a number of quantum chemistry approaches [6, 11–21]. Lately, the DFT scheme has been acknowledged as appropriate for the study of this polymer as a number of research groups have provided evidence that it renders accurate description [22–31]. Furthermore, the implementation of the DFT scheme is the only inexpensive way of accounting to a decent extent the electron correlation in systems of this size. The majority of the published quantum chemistry results do not estimate the influence of the solvent on the structure and properties of the emeraldine salt; therefore, the simulations are usually made in vacuum, in spite of the abovementioned arguments for the significance of the solvent's nature. Nevertheless, there are a limited number of studies in which the solvent is part of the modeled system. In these, PANI is treated mostly with semiempirical methods, and the explicit solvent is described at the same or lower level of theory (molecular mechanics, semiempirical) [32–38] or is introduced implicitly (PCM, COSMO) [19, 39, 40]. In preceding studies based on the DFT approach [41], we have demonstrated that the impact of the electrostatic interactions emeraldine salt–solvent may be evaluated reliably by means of implicit aqueous medium representation—PCM [42, 43]. Moreover, some significant drawbacks (unrealistic spin density at Cl^-, alongside with low charge) of the simulation of emeraldine–HCl in vacuum are removed with introduction of polar environment (Supporting Information Table S1). These studies also outline a number of advantages of the BLYP functional for description of the system in comparison to other methods and the satisfactory performance of the 6-31G* basis set for the study of this target. Thus, the current calculations are carried out with BLYP/6-31G*/PCM.

In this investigation, we model PANI salts originating from the emeraldine base, which differ solely in the kind of protonating agents used. The latter are inorganic—HCl, HBr, and H_2SO_4 and organic—HMSA, HBSA, and CSA. The computational protocol comprises full geometry optimization of six tetramer emeraldine salts, each of them represented by their bipolaron (singlet) and polaron (two polarons in triplet configuration) forms. Various implicit solvents are used: water, $\varepsilon = 78.35$ (HCl, HBr, H_2SO_4, and CSA),

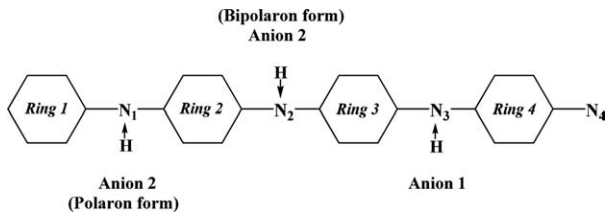

FIGURE 2. Schematic representation of the fragments in a NH_2-terminated tetramer model of emeraldine salt in bipolaron (protonation at N2 and N3) and polaron (protonation at N1 and N3) forms.

chloroform, $\varepsilon = 4.71$ (MSA, BSA, and CSA), and *m*-cresol, $\varepsilon = 12.44$ (CSA). With the aim of revealing the doping effect on the emeraldine base, a tetramer base model is optimized with the same functional, basis set, and solvents. All singlets are computed with the restricted version of the method and all triplets with the unrestricted one. Each structure is subject to frequency analysis and is in energy minimum with respect to the atomic coordinates. The electron density distribution is taken from NBO [44] analysis.

All calculations are made with Gaussian 09 [45]. The latest version of the Gaussian program suit implements an improved procedure for geometry optimization in PCM, ensuring shorter computation times and faster convergence.

Results and Discussion

As prime descriptor of the medium effect and the influence of the proton acid doping agent on the molecular geometry of the emeraldine salts is selected the bond-length alternation (BLA). This parameter is calculated for the molecular fragments, which are presented schematically in Figure 2, for the two forms (bipolaron and polaron). In our models, these differ in the position of the second protonated site (balanced by Anion 2), in accordance with the proposed molecular structures [6]. In the ring fragments, the BLA is calculated by subtraction of the averaged "single" C—C bonds from the averaged "double" C—C bonds (the latter being the ones parallel to the polymer axis). The BLA values for the optimized structures of the tetramer emeraldine base, the bipolaron and polaron forms of the different salts, are summarized in Figure 3. The BLA of the fragments in the base depends insignificantly on solvent polarity (Supporting Information Table S2), and therefore averaged BLA data from the results in different solvents are presented for the base.

The comparison of the different bipolaron forms (Fig. 3, left) makes it clear that the changes of the base geometry invoked by protonation are qualitatively the same. The BLA decreases markedly in the quinoid ring and at the imine nitrogens, whereas in the aromatic rings and at the amine nitrogens it increases sizably. This tendency is observed in all cases, irrespective of the protonating agent or the solvent polarity. With the exception of the aromatic ring at the phenyl end, the structural defect spans the entire remaining portion of the molecule, including the terminal NH_2 group (Supporting Information Table S3). The results obtained for the length and

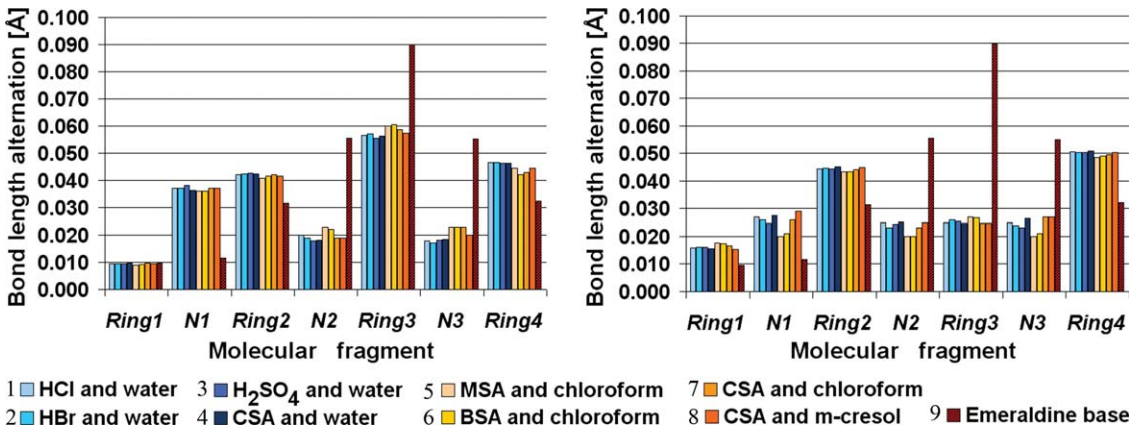

FIGURE 3. Bond length alternation (Å) of the molecular fragments in the emeraldine base (rightmost bar in the dataset for each fragment in both panels) and the bipolaron (left) and polaron (right) forms of the emeraldine salts with various dopants (labels 1–8 correspond to bars from left to right), calculated with BLYP/6-31G*/PCM. [Color figure can be viewed in the online issue, which is available at wileyonlinelibrary.com.]

TABLE I

BLYP/6-31G*/PCM group NBO charges of fragments (Fig. 2) in the bipolaron form of the tetramer emeraldine salt for different dopant/solvent combinations.

Solvent	Water				Chloroform			*m*-Cresol
Dopant	HCl	HBr	H_2SO_4	CSA	MSA	BSA	CSA	CSA
Ring1	0.216	0.215	0.221	0.216	0.205	0.208	0.215	0.216
N1	−0.064	−0.064	−0.061	−0.063	−0.081	−0.079	−0.075	−0.067
Ring2	0.464	0.461	0.475	0.463	0.453	0.458	0.468	0.466
N2	−0.025	−0.033	0.005	0.003	0.007	0.006	0.011	0.006
Ring3	0.541	0.533	0.546	0.539	0.559	0.560	0.550	0.543
N3	−0.019	−0.027	0.010	0.005	0.013	0.013	0.008	0.006
Ring4	0.457	0.453	0.460	0.454	0.444	0.446	0.432	0.445
N4	0.157	0.156	0.160	0.155	0.133	0.134	0.122	0.143
Anion 1	−0.864	−0.846	−0.907	−0.888	−0.866	−0.873	−0.866	−0.880
Anion 2	−0.864	−0.847	−0.907	−0.884	−0.866	−0.872	−0.866	−0.877

geometry of the bipolaron defects correlate with our earlier results [41] and with experimental data for the single crystal emeraldine salt [7]. On the other hand, the electron structure of the defect (see also below) corresponds to the models suggested by Stafström et al. [6] for the RU of a bipolaron PANI lattice. Minor BLA variations in the region of the protonated nitrogens and the ex-quinoid ring can be noticed for the different combinations of proton donors and solvents. Organic dopants in chloroform tend to keep a little bit higher BLA in these fragments, but no definite relationship can be outlined.

Juxtaposition of the polaron forms in the selected combinations of counterions and solvents (Fig. 3, right) reveals inconsequential differences. In all cases, the BLA of the ex-quinoid ring (Ring3) decreases substantially at the expense of an increase in the adjacent rings. A new feature is the partial involvement of the terminal phenyl ring in the defect in contrast to the bipolaron forms. Alternation of rings with more expressed aromatic and more pronounced quinoid character is observed in the polaron forms (two polaron defects) alongside with equalization of the nitrogen atoms. However, distinct reduction of the tetramer RU to a dimer one, as suggested by other authors [6], cannot be established in our model, because of the less marked changes in the terminal phenyl ring. Nevertheless, the witnessed changes are in the correct direction, and the absence of RU dimerization is most probably due to end effects. In overall, the polaron forms exhibit smaller BLA variations along the chain than the bipolaron ones. The BLA of the high-spin systems also differs slightly depending on the dopant/solvent combination. Here, mainly the N-fragments are affected, for example, MSA and BSA in chloroform invoke somewhat lower BLA but again no strict rules can be postulated.

The BLYP/6-31G*/PCM group NBO charges of each fragment (see Fig. 1) of the bipolaron and polaron forms of the salts under consideration are presented in Tables I and II, respectively.

The charge distribution fully agrees with the BLA values for the bipolarons. In all singlet salts, the positive charge is highest in the ex-quinoid ring of the base (Ring3, Table I). Comparative analysis reveals that the charge distribution in all spinless emeraldine salts within the same solvent is analogous. Small charge variations are observed at the protonated nitrogens. When the dopant is an oxygen-containing acid, the electron density at the protonated N-fragments is lowered in correspondence with the distance proton-counterion (Supporting Information Table S4a). In general, the raise of solvent polarity negligibly enhances the delocalization of positive charge toward the NH_2 end of the chain.

The polaron form of the salts also features comparable group charge distribution matching the BLA results (Table II). The electron density at the rings neighboring the ex-quinoid one of the base (Ring3) is lower than that in Ring3 itself, but overall the electron density is more uniformly distributed among the three rings than in the bipolaron form. This clearly shows a qualitatively different charge partitioning scheme compared

TABLE II

BLYP/6-31G*/PCM group NBO charges of fragments (Fig. 2) in the polaron form of the tetramer emeraldine salt for different dopant/solvent combinations.

Solvent	Water				Chloroform			*m*-Cresol
Dopant	HCl	HBr	H_2SO_4	CSA	MSA	BSA	CSA	CSA
Ring1	0.277	0.274	0.285	0.272	0.293	0.296	0.286	0.276
N1	−0.035	−0.044	−0.009	−0.012	0.000	0.001	−0.001	−0.008
Ring2	0.498	0.491	0.502	0.499	0.484	0.488	0.489	0.496
N2	−0.049	−0.050	−0.047	−0.049	−0.069	−0.068	−0.069	−0.057
Ring3	0.427	0.423	0.435	0.423	0.423	0.426	0.420	0.422
N3	−0.044	−0.053	−0.019	−0.021	−0.012	−0.012	−0.012	−0.018
Ring4	0.492	0.484	0.496	0.493	0.467	0.471	0.477	0.487
N4	0.182	0.180	0.185	0.181	0.151	0.153	0.150	0.170
Anion 1	−0.874	−0.851	−0.914	−0.891	−0.869	−0.877	−0.869	−0.883
Anion 2	−0.874	−0.854	−0.914	−0.894	−0.868	−0.877	−0.871	−0.886

with the low-spin analogs and indicates the tendency toward separation of the highest charge-loaded centers in the polaron form. In the high-spin state of the latter, the charge is much better delocalized along the chain in comparison to the bipolaron models. When the dopant is an oxygen-containing acid, the electron density at the protonated fragments (N1 and N3) is lowered and at the nonprotonated (N2, N4) is raised. Some petty increase of the positive charge in Ring2 and the terminal monomer unit (Ring4, N4) and decrease in Ring1 is observed with growth of solvent polarity.

In addition to the charge distribution, the Mulliken atomic spin densities of the high-spin forms are estimated and summed for each fragment (Table III, the counterions have zero spin density and are not presented). As with the electron density, the spin density does not seem to be very sensitive to the dopant/solvent pair. Highest values of spin density feature Ring4 and Ring2, the remaining two rings being loaded with approximately twice as low spin. All N-fragments also carry some spin density, being higher at the protonated sites. Such spin density distribution indicates the tendency toward separation of the two polarons in the oligomer chain. Slight increase of the spin density in the terminal monomer unit (Ring4-N4) and decrease in the phenyl end (Ring1-N1) with increase of solvent polarity can be registered. The atomic spin density preserves positive values in all fragments except in Ring 1 where spin polarization is found (Supporting Information Table S5).

The relative stability of the two spin forms is compared on the basis of total energy calculations.

TABLE III

BLYP/6-31G*/PCM group Mulliken spin densities of fragments (Fig. 2) in the polaron form of the tetramer emeraldine salt for different dopant/solvent combinations.

Solvent	Water				Chloroform			*m*-Cresol
Dopant	HCl	HBr	H_2SO_4	CSA	MSA	BSA	CSA	CSA
Ring1	0.180	0.186	0.188	0.188	0.212	0.210	0.204	0.185
N1	0.262	0.256	0.258	0.268	0.281	0.280	0.284	0.272
Ring2	0.357	0.352	0.358	0.356	0.347	0.348	0.352	0.360
N2	0.172	0.171	0.174	0.170	0.156	0.157	0.157	0.167
Ring3	0.215	0.219	0.220	0.213	0.227	0.225	0.214	0.213
N3	0.252	0.247	0.246	0.259	0.264	0.264	0.271	0.261
Ring4	0.419	0.412	0.421	0.417	0.399	0.402	0.405	0.416
N4	0.205	0.202	0.208	0.201	0.182	0.184	0.183	0.198

TABLE IV

Energy difference, $\Delta E_{\text{bipol-pol}}$ (kcal/mol), between the total energies of the bipolaron form of the singlet and the polaron triplet form of the respective tetramer emeraldine salt calculated with BLYP/6-31G*/PCM.

Solvent	Water				Chloroform			*m*-Cresol
Dopant	HCl	HBr	H_2SO_4	CSA	MSA	BSA	CSA	CSA
$\Delta E_{\text{bipol-pol}}$	−8.71	−8.86	−8.59	−8.55	−11.19	−10.97	−10.94	−9.54

The results for the total energy difference between the bipolaron and the polaron form for each dopant/solvent pair are shown in Table IV. Negative sign of $\Delta E_{\text{bipol-pol}}$ means more stable low-spin form.

The $\Delta E_{\text{bipol-pol}}$ results prove that the bipolaron form is more stable at any combination of dopant and solvent for the tetramer. A possible reason for the dominance of the bipolaron may be the insufficient length of the tetramer chain for equitable distribution of the two polarons. As seen from the above data, in the polaron forms, the defect tends but fails to propagate entirely to the phenyl-end ring. Thus, the polaron form becomes less stable. It is obvious that $\Delta E_{\text{bipol-pol}}$ decreases with increase of the dielectric permittivity of the solvent. Within the same solvent, the change of dopant has insignificant effect on the relative stability at the tetramer level.

Additional information on the solvent effect is supplied by the dipole moments of the two forms of the salts (Table V). In all considered cases, the polaron form is distinctly more polar than the bipolaron one. This explains the finding that with increase of solvent's polarity, the stability of the polaron form grows and $\Delta E_{\text{bipol-pol}}$ lessens (Table V). This is illustrated well by the PANI–CSA results for different solvents. Apparently, the polarity of the salts, especially of their bipolaron forms, depends on the dopant kind. For instance, in aqueous solution, the dipole moment of the bipolaron CSA salt is an order of magnitude higher than those of the inorganic acid salts. Therefore, it could be expected that the optical characteristics of the studied bipolaron salts in water would differ, as their ground state will be stabilized to a nonidentical extent by the polar environment.

Conclusions

The results of the performed model calculations allow to conclude that the molecular structure and the electron density distribution of the bipolaron and polaron forms of the emeraldine salt do not depend on the kind of protonating agent: in all bipolaron forms, the largest positive charge is localized at the ex-quinoid ring of the base, wherein the quinoid character is blurred but not lost upon protonation; in the polaron forms, the lowest electron and the highest spin density are concentrated in the rings adjacent to the ex-quinoid one, accompanied by pronounced dearomatization of these rings. The present theoretical treatment outlines the solvent polarity as the major factor invoking the mild structural differences between the salts. High dielectric permittivity of the medium favors the process of primary doping and stabilizes the polaron forms. The presented results, however, are insufficiently particulate to reflect the secondary doping effect.

TABLE V

BLYP/6-31G*/PCM dipole moments, $\mu(D)$, based on the Mulliken population analysis of the bipolaron (singlet) and polaron (triplet) forms of tetramer emeraldine salts in the respective solvent.

Solvent	Water				Chloroform			*m*-Cresol
Dopant	HCl	HBr	H_2SO_4	CSA	MSA	BSA	CSA	CSA
μ (Singlet)	0.75	0.68	1.12	10.93	8.72	9.11	8.13	9.73
μ (Triplet)	39.27	38.96	39.79	41.17	31.61	32.31	35.11	38.05

This permits us to summarize that the electrostatic interactions with the solvent included in our model cannot fully decipher the empirically observed relationships. Implementation of explicit solvent is necessary for a more detailed study of the dopant–PANI–medium interactions. The account of the chemical structure of the medium would reveal specific intermolecular interactions that would bring about new insight in the interpretation of the structure and properties of the emeraldine salts. This will be the next step of our research.

ACKNOWLEDGMENT

The authors thank Dr. Anela Ivanova and Jasmina Petrova for the helpful discussion.

References

1. (a) Epstein, A. J.; Ginder, J. M.; Zuo, F.; Bigelow, R. W.; Woo, H.-S.; Tanner, D. B.; Richter, A. F.; Huang, W.-S.; MacDiarmid, A. G. Synth Met 1987, 18, 303; (b) Lee, K.; Cho, S.; Park, S. H.; Heeger, A. J.; Lee, C. W.; Lee, S. H. Nature 2006, 441, 65.
2. Huang, W.-S.; MacDiarmid, A. G. Polymer 1993, 34, 1833.
3. Wei, Y.; Jang, G. W.; Hsueh, K. F.; Scherr, E. M.; MacDiarmid, A. G.; Epstein, A. J. Polymer 1992, 33, 314.
4. (a) Gospodinova, N.; Terlemezyan, L. Prog Polym Sci 1998, 23, 1443; (b) Pron, A.; Rannou, P. Prog Polym Sci 2002, 27, 135; (c) Bhadra, S.; Khastgir, D.; Singha, N. K.; Lee, J. H. Prog Polym Sci 2009, 34, 783.
5. (a) Chiang, J. C.; MacDiarmid, A. G. Synth Met 1986, 13, 193; (b) MacDiarmid, A. G.; Chiang, J. C.; Richter, A. F.; Epstein, A. J. Synth Met 1987, 18, 285.
6. Stafström, S.; Brédas, J. L.; Epstein, A. J.; Woo, H. S.; Tanner, D. B.; Huang, W. S.; MacDiarmid, A. G. Phys Rev Lett 1987, 59, 1464.
7. Shacklette, L. W.; Wolf, J. F.; Gould, S.; Baughman, R. H. J Chem Phys 1988, 88, 3955.
8. Mu, S.; Kan, J. Synth Met 1998, 98, 51; (b) Kang, E. T.; Neoh, K. G.; Woo, Y. L.; Tan, K. L. Polymer 1992, 33, 2857.
9. Joe, J.; Chung, Y. C.; Song, H. G.; Baeck, J. S.; Lee, W. P.; Epstein, A. J.; MacDiarmid, A. G.; Jeong, K.; Oh, E. J. Synth Met 1997, 84, 739.
10. MacDiarmid, A. G.; Epstein, A. J. Synth Met 1995, 69, 85.
11. Chance, R. R.; Boudreaux, D. S.; Wolf, J. F.; Shacklette, L. W.; Silbey, R.; Themans, B.; Andrec, J. M.; Brédas, J. L. Synth Met 1986, 15, 105.
12. Stafström, S.; Sjögren, B.; Wennerström, O.; Hjertberg, T. Synth Met 1986, 16, 31.
13. Stafström, S. Synth Met 1991, 43, 3697.
14. Libert, J.; Brédas, J. L.; Epstein, A. J. Phys Rev B 1995, 51, 5711.
15. Libert, J.; Brédas, J. L. Synth Met 1995, 69, 121.
16. Libert, J.; Cornil, J.; dos Santos, D. A.; Brédas, J. L. Phys Rev B 1997, 56, 8638.
17. Barta, P.; Kugler, Th.; Salaneck, W. R.; Monkman, A. P.; Libert, J.; Lazzaroni, R.; Brédas, J. L. Synth Met 1998, 93, 83.
18. de Oliveira, Z. T., Jr.; dos Santos, M. C. Solid State Commun 2000, 114, 49.
19. de Oliveira, Z. T., Jr.; dos Santos, M. C. Chem Phys 2000, 260, 95.
20. Lim, S. L.; Tan, K. L.; Kang, E. T.; Chin, W. S. Chem Phys 2000, 112, 10648.
21. Kwon, O.; McKee, M. L. J Phys Chem B 2000, 104, 1686.
22. Cavazzoni, C.; Colle, R.; Farchioni, R.; Grosso, G. Phys Rev B 2002, 66, 165110.
23. Foreman, J. P.; Monkman, A. P. J Phys Chem A 2003, 107, 7604.
24. Cavazzoni, C.; Colle, R.; Farchioni, R.; Grosso, G. Phys Rev B 2004, 69, 115213.
25. Cavazzoni, C.; Colle, R.; Farchioni, R.; Grosso, G. Comp Phys Commun 2005, 169, 135.
26. Varela-Ávarez, A.; Sordo, J. A.; Scuseria, G. E. J Am Chem Soc 2005, 127, 11318.
27. Cavazzoni, C.; Colle, R.; Farchioni, R.; Grosso, G. Phys Rev B 2006, 74, 033103.
28. Colle, R.; Parruccini, P.; Benassi, A.; Cavazzoni, C. J Phys Chem B 2007, 111, 2800.
29. Alemán, C.; Ferreira, C. A.; Torras, J.; Meneguzzi, A.; Canales, M.; Rodrigues, M. A. S.; Casanovas, J. Polymer 2008, 49, 5169.
30. Yang, G.; Hou, W.; Feng, X.; Jiang, X.; Guo, J. Int J Quantum Chem 2008, 108, 1155.
31. Varela-Ávarez, A.; Sordo, J. A. J Chem Phys 2008, 128, 174706.
32. Ivanova, A.; Madjarova, G.; Tadjer, A.; Gospodinova, N. Int J Quantum Chem 2006, 106, 1383.
33. Zhekova, H.; Tadjer, A.; Ivanova, A.; Petrova, J.; Gospodinova, N. Int J Quantum Chem 2007, 107, 1688.
34. Gospodinova, N.; Dorey, S.; Ivanova, A.; Zhekova, H.; Tadjer, A. Int J Polym Anal Charact 2007, 12, 251.
35. Ivanova, A.; Tadjer, A.; Gospodinova, N. J Phys Chem B 2006, 110, 2555.
36. Shacklette, L. W. Synth Met 1994, 65, 123.
37. Lee, K. H.; Park, B. J.; Song, D. H.; Chin, I. J.; Choi, H. J. Polymer 2009, 50, 4372.
38. Ikkaala, O. T.; Piefilä, L.-O.; Passiniemi, P.; Vikki, T.; Österholm, H.; Ahjopalo, L.; Österholm, J.-E. Synth Met 1997, 84, 55.
39. Ćirić-Marjanović, G.; Trchová, M.; Stejskal, J. Collect Czech Chem Commun 2006, 71, 1407.
40. (a) Ćirić-Marjanović, G.; Trchová, M.; Stejskal, J. Int J Quantum Chem 2008, 108, 318; (b) Ćirić-Marjanović, G.; Konyushenko, E. N.; Trchová, M.; Stejskal, J. Synth Met 2008, 158, 200.
41. (a) Romanova, J.; Petrova, J.; Tadjer, A.; Gospodinova, N. Synth Met (in press); DOI: 10.1016/j.synthmet. 2010.02.025; (b) Romanova, J.; Petrova, J.; Ivanova, A.; Tadjer, A.; Gospodinova, N. J Mol Struct: THEOCHEM; DOI: 10.1016/j.theochem. 2010.01.032.

42. Miertuš, S.; Scrocco, E.; Tomasi, J. Chem Phys 1981, 55, 117.
43. Tomasi, J.; Mennucci, B.; Cammi, R. Chem Rev 2005, 105, 2999.
44. (a) Foster, J. P.; Weinhold, F. J Am Chem Soc 1980, 102, 7211; (b) Reed, A. E.; Weinhold, F. J Chem Phys 1983, 78, 4066; (c) Reed, A. E.; Weinstock, R. B.; Weinhold, F. J Chem Phys 1985, 83, 735; (d) Reed, A. E.; Weinhold, F. J Chem Phys 1985, 83, 1736; (e) Carpenter, J. E.; Weinhold, F. J Mol Struct (Theochem) 1988, 46, 41; (f) Reed, A. E.; Curtiss, L. A.; Weinhold, F. Chem Rev 1988, 88, 899.
45. Frisch, M. J.; Trucks, G. W.; Schlegel, H. B.; Scuseria, G. E.; Robb, M. A.; Cheeseman, J. R.; Scalmani, G.; Barone, V.; Mennucci, B.; Petersson, G. A.; Nakatsuji, H.; Caricato, M.; Li, X.; Hratchian, H. P.; Izmaylov, A. F.; Bloino, J.; Zheng, G.; Sonnenberg, J. L.; Hada, M.; Ehara, M.; Toyota, K.; Fukuda, R.; Hasegawa, J.; Ishida, M.; Nakajima, T.; Honda, Y.; Kitao, O.; Nakai, H.; Vreven, T.; Montgomery, J. A., Jr.; Peralta, J. E.; Ogliaro, F.; Bearpark, M.; Heyd, J. J.; Brothers, E.; Kudin, K. N.; Staroverov, V. N.; Kobayashi, R.; Normand, J.; Raghavachari, K.; Rendell, A.; Burant, J. C.; Iyengar, S. S.; Tomasi, J.; Cossi, M.; Rega, N.; Millam, J. M.; Klene, M.; Knox, J. E.; Cross, J. B.; Bakken, V.; Adamo, C.; Jaramillo, J.; Gomperts, R. E.; Stratmann, O.; Yazyev, A. J.; Austin, R.; Cammi, C.; Pomelli, J. W.; Ochterski, R.; Martin, R. L.; Morokuma, K.; Zakrzewski, V. G.; Voth, G. A.; Salvador, P.; Dannenberg, J. J.; Dapprich, S.; Daniels, A. D.; Farkas, O.; Foresman, J. B.; Ortiz, J. V.; Cioslowski, J.; Fox, D. J. Gaussian 09, Revision A. 02; Gaussian, Inc.: Wallingford, CT, 2009.